Analytica Chimica Acta 765 (2013) 63–69

Contents lists available at SciVerse ScienceDirect

Analytica Chimica Acta

journal homepage: www.elsevier.com/locate/aca

Novel electrochemical biosensor based on functional composite nanofibers for sensitive detection of p53 tumor suppressor gene

Xiaoying Wang[a,*], Xiaobing Wang[b], Xiaoning Wang[c], Fentian Chen[a], Kehui Zhu[a], Qian Xu[a], Meng Tang[a]

[a] Key Laboratory of Environmental Medicine and Engineering, Ministry of Education, School of Public Health, Southeast University, Nanjing 210009, China
[b] Department of Natural Medicinal Chemistry, China Pharmaceutical University, Nanjing 210009, China
[c] Department of Hematology, The First Affiliated Hospital of Xi' an Jiao Tong University, Xi' an 710061, China

HIGHLIGHTS

- A novel electrochemical p53 biosensor based on functional composite nanofibers (MWNTs–PA6–PPy) was developed.
- The MWNTs–PA6–PPy electrode with large specific surface area and good biocompatibility can be used to enhance stability, speed and sensitivity.
- The biosensor can detect 50 fM wild type p53 sequence.
- The strategy could be extended to develop various sensors for the detection of many kinds of analytes.

GRAPHICAL ABSTRACT

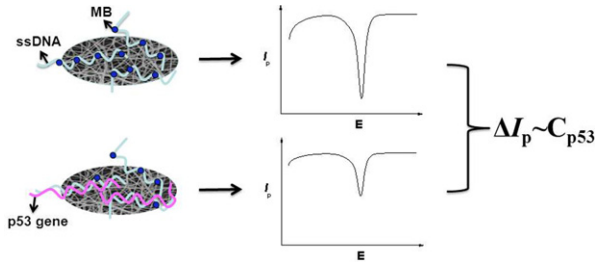

ARTICLE INFO

Article history:
Received 1 November 2012
Received in revised form
14 December 2012
Accepted 20 December 2012
Available online 31 December 2012

Keywords:
Functional composite nanofibers
Electrospinning
Methylene blue
Wild type p53 sequence
Mutant type p53 sequence

ABSTRACT

A novel electrochemical biosensor based on functional composite nanofibers for sensitive hybridization detection of p53 tumor suppressor using methylene blue (MB) as an electrochemical indicator is developed. The carboxylated multi-walled carbon nanotubes (MWNTs) doped nylon 6 (PA6) composite nanofibers (MWNTs–PA6) was prepared using electrospinning, which served as the nanosized backbone for pyrrole (Py) electropolymerization. The functional composite nanofibers (MWNTs–PA6–PPy) used as supporting scaffolds for ssDNA immobilization can dramatically increase the amount of DNA attachment and the hybridization sensitivity. The biosensor displayed good sensitivity and specificity. The target wild type p53 sequence (wtp53) can be detected as low as 50 fM and the discrimination is up to 57.5% between the wtp53 and the mutant type p53 sequence (mtp53). It holds promise for the early diagnosis of cancer development and monitoring of patient therapy.

1. Introduction

The p53 tumor suppressor gene located on chromosome 17 p13 contains 11 exons spanning 20 kilobases and encodes a (mostly) nuclear phosphoprotein of 53 kD [1]. In human tumors, it is the most commonly mutated gene which may lead to the loss of transcriptional activation potency and the ability to bind DNA. About half of the cancers contain a mutation in p53. Moreover, p53 is involved in sustaining cellular homeostasis and in complex regulatory interactions [2,3]. Sequence-specific analysis of the p53 could help early diagnosis of cancer and consequently increase the success of the treatment [4,5]. Therefore, specific recognition

* Corresponding author. Tel.: +86 25 83272563; fax: +86 25 83272561.
E-mail address: wxy@seu.edu.cn (X. Wang).

0003-2670/$ – see front matter © 2012 Elsevier B.V. All rights reserved.
http://dx.doi.org/10.1016/j.aca.2012.12.037

and quantitative detection of p53 and the mutations in the p53 are extremely crucial in fundamental research and clinical practice.

Thus far, a variety of methods for measuring p53 tumor suppressor gene have been reported. One aims at finding unknown mutations in candidate or known disease genes, such as the direct DNA sequencing technology [6]. Others aim at finding known mutations, preferably with high throughput, such as the denaturing high-performance liquid chromatography (DHPLC) [7], the single-strand conformation polymorphism (SSCP) [8], and the denaturing gradient gel electrophoresis (DGGE), etc. [9,10]. However, these approaches are time consuming, highly skilled labor, less sensitive and expensive equipment [11]. Two common methods, the electrophoretic mobility shift assay (EMSA) and enzyme-linked immunosorbant assay (ELISA) were employed later. The former is simple but is semiquantitative at best, whereas the latter is sensitive but requires the use of p53 antibodies and measures only the total p53 (i.e., wild type and mutant type combined) [12]. Recently, the DNA-based biosensor for the detection of p53 mutations has generated considerable interest for simple, rapid and inexpensive testing of genetic and infectious diseases [13]. The sensors intimately combine a specific type of DNA, serving as a biological recognition molecule, with electrochemical [14–16], piezoelectric [17], optical [18,19] and electrochemiluminescence [20] transducers to translate the genetic recognition event into a corresponding analytical signal. Among them, electrochemical techniques allow the development of extremely sensitive and accurate, yet simple, inexpensive, real-time and robust gene-sensing platforms [21]. As an important factor to develop an electrochemical biosensor device, the amount and stability of the biological recognition molecule was very vital. Although the field of electrochemical biosensors has grown considerably and a great number of different detection methods and strategies are available in the past decade, the researchers still think it is a big challenge that how to make the biological recognition molecule utmost and stability immobilizing on the supporting scaffolds [21,22].

Nanomaterials have received increasing attention for their unique physical and chemical properties. Compared to conventional planar materials, the nanofibers produced by electrospinning processes have several advantages including uniformity, porosity, mechanical strength and large surface areas [23,24]. Many studies have utilized electrospun nanofibers for biomedical and industrial applications, such as the supporting scaffolds for enzyme immobilization [25], the membranes for filtration [26], the tissue templates [27], the artificial organ implant and the drug delivery [28]. It is believed that electrospun nanofibers can be used as an ideal platform for highly sensitive biosensing applications, with all of the aforementioned advantages, including high surface area for loading, capability of functional immobilization with desired spacing, reproducibility and long-term storage [29]. Several reports have investigated the development of nanofiber-based biosensing platforms for biomolecular detection, such as glucose [30], protein [31] and DNA [32]. But biosensor based on electrospun nanofibers has never been applied to detect the p53 tumor suppressor.

Nylon 6 (PA6), a major class of engineering plastics, is a semiconducting polymer. The electrospun PA6 nanofibers have extensive range of applications owing to the outstanding durability, chemical and abrasion resistance [33]. The blends of PA6 with carbon nanotubes have commercial interest because of the unique mechanical and electrical properties of carbon nanotubes and its contribution to the blend's dimensional stability, processability and high toughness. However, the lack of biological affinity is one apparent and critical disadvantage of the carbon nanotubes doped PA6 composite nanofibers in biomolecule recognition [34,35]. Thus, the biocompatibility functionalized of the composite nanofibers has come to significant attraction.

The aim of the present work is to develop a high sensitivity electrochemical biosensor for the determination of p53 tumor suppressor based on functional composite nanofibers using methylene blue (MB) as an electrochemical indicator. The carboxylated multi-walled carbon nanotubes (MWNTs) doped nylon 6 (PA6) composite nanofibers (MWNTs–PA6) was prepared using electrospinning, which served as the nanosized backbone for pyrrole (Py) electropolymerization. The functional composite nanofibers (MWNTs–PA6–PPy) with large specific surface area and good biocompatibility used as supporting scaffolds for ssDNA immobilization can dramatically increase the amount of DNA attachment and the hybridization sensitivity. The experimental protocol is illustrated in Fig. 1. In this paper, the characteristics of the sensing system for the detection of p53 mutations and the analytical performance were performed.

2. Experiment

2.1. Reagents and apparatus

The DNA oligonucleotides were obtained from Sangon Biotechology Inc. (China). Wide type p53 (wtp53): 5′-GGCACAAACACGCACCTCAA-3′, mutant type p53 (mtp53): 5′-GGCACAAACA*T*GCACCTCAA-3′, the ssDNA (complementary sequence of the wtp53): 5′-HS-$(CH_2)_6$-AAATTGAGGTGCGTGTTTGTGCC-3′, three-base mismatched sequence of the wtp53: 5′-GGC*T*CAAA*G*ACGCACC*A*CAA-3′, noncomplementary sequence of the wtp53: 5′-*TTGTGCCCTGTATGGGGAGC*-3′ (italic and underlined nucleotide is the mismatched base). Pyrrole monomer (>99%), nylon 6 (PA6) and methylene blue (MB) were purchased from Sigma (USA). Carboxylated multi-walled carbon nanotubes (MWNTs) were obtained from Shenzhen Nanotech Port Co. Ltd. (China). The diameter was 40–60 nm and the length 1–10 μm. Other reagents were of analytical reagent grade. All the solutions were prepared with ultrapure water from a Millipore Milli-Q system.

The field-emission scanning electron microscope (FESEM) images were recorded using S-4800 FE-SEM (JEOL, Japan). A CHI 660D electrochemical analyzer (CHI instruments Inc., Chenhua Corp., China) was used to carry out differential pulse voltammetry (DPV), cyclic voltammogram (CV) and electrochemical impedance spectroscopy (EIS). A three-electrode system was used with the modified Au electrode (2 mm in diameter) as the working electrode, an Ag/AgCl (sat.) as the reference electrode and a platinum wire as the counter electrode.

2.2. Preparation of functional composite nanofibers

The surface of Au electrode was polished with alumina slurry, rinsed with water and ethanol in an ultrasonic bath briefly. The Au electrode was further treated electrochemically in 0.5 M H_2SO_4 by scanning the potential from −0.2 V to 1.7 V with a scan rate of 10 V s^{-1} for 15 min until an ideal voltammogram was observed. PA6 and MWNTs (0.1% of PA6) were dissolved in mixture of cresol and formil acid (6:4, v/v) to obtain a homogeneous solution under vigorous stirring at room temperature. Electrospinning was carried out with a 20 mL syringe (1.2 mm diameter spinneret) at electrical potential of 15 kV over a 15 cm gap between the spinneret and the cleaned Au surface with a rate of 1.0 mL h^{-1}. The ambient temperature and relative humidity for electrospinning were kept at 25 °C and 40%, respectively. It took 3 min to deposit the nanofibrous mat on the surface of the electrode. The as-prepared electrode was denoted as MWNTs–PA6 electrode.

The electrode was dipped into 0.05 M pyrrole solution containing 0.1 M KCl–HCl (pH 3.0) to carry out CV in range of 0.0 to

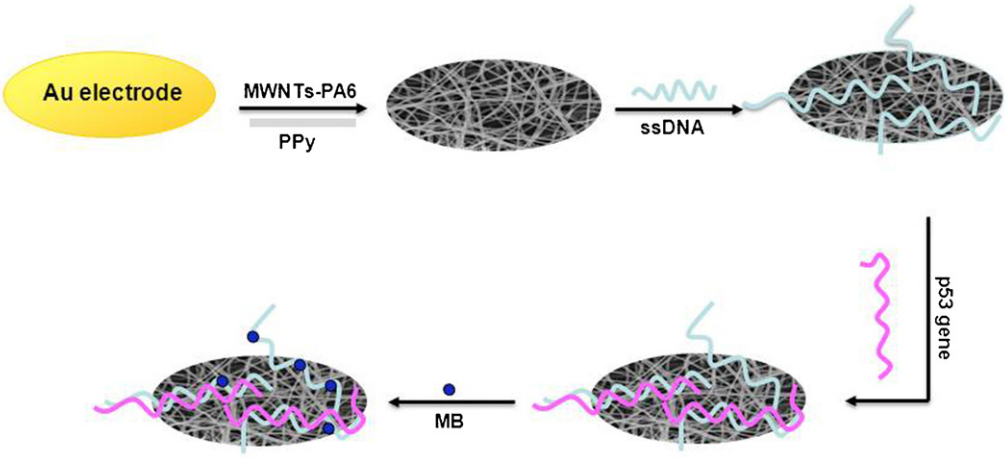

Fig. 1. Schematic representation of the preparation of the electrochemical biosensor.

+0.7 V (vs. Ag/AgCl) for 8 cycles with a scan rate of 50 mV s^{-1}. A modest stir was going on through the electropolymerization. The MWNTs–PA6–PPy was formed on the Au electrode surface.

2.3. Fabrication of the electrochemical biosensing electrode

The MWNTs–PA6–PPy electrode was immersed into 0.1 M HAc solution (pH 5.4) containing 1 μM ssDNA, and a constant potential at +0.5 V (vs. Ag/AgCl) for 400 s was applied. Then the electrode was rinsed with 10 mM PBS (pH 7.3), and the ssDNA electrode was formed.

The ssDNA electrode was immersed into 10 mM PBS (pH 7.3, 0.5 M NaCl) containing p53 sequence at 40 °C for 40 min. Then it was washed with 10 mM PBS (pH 7.3) to remove the unhybridized p53. By this way, the dsDNA electrode was obtained.

In order to accumulate MB onto dsDNA, the dsDNA electrode was incubated with 50 mM Tris–HCl (pH 8.0, 20 μM MB) under stirring for 8 min. The electrode was washed with 0.5% SDS solution to remove the residual adsorbed DNA and hybrid on the electrode surface thoroughly according to the literature [36], and then washed with the ultrapure water. The dsDNA–MB electrode was obtained and employed as working electrode to detect DPV signal.

2.4. Measurement

The DPV measurements were conducted from −0.1 V to −0.70 V in 40 mM Tris–HCl (pH 8.0, 20 mM NaCl) with pulse amplitude 0.05 V, pulse width 0.05 s and pulse period 0.2 s. The peak current related to the reduction of MB at about −0.32 V was taken as the electrochemical measurement signal.

3. Results and discussion

3.1. FESEM image of MWNTs–PA6 composite nanofibers and MWNTs–PA6–PPy electrode

The micro-morphologies of MWNTs–PA6 composite nanofibers and MWNTs–PA6–PPy electrode were analyzed using FESEM as shown in Fig. 2. MWNTs–PA6 composite nanofibers with smooth surface are evenly distributed on the substrate, and their orientations are random. The diameters of the nanofibers range from 50 nm to 300 nm (Fig. 2A). A 3D porous and dense modification layer on the electrode surface was obtained for MWNTs–PA6–PPy electrode (Fig. 2B). Quantitative estimation of the average pore diameter of the above nanofibers was performed. Compared with the MWNTs–PA6 composite nanofibers, the average pore diameter of the MWNTs–PA6–PPy electrode decreased from 0.37 μm to 0.20 μm. In this case, MWNTs–PA6 composite nanofibers served as the nanosized backbone for Py polymerization, resulting in the porous PPy film covered around the MWNTs–PA6 composite nanofibers in a cylinder structure. By this way, a significantly increasing of the PPy amount around MWNTs–PA6 composite nanofibers was generated. Finally, the MWNTs–PA6–PPy electrode with coarser nanofibers and a smaller pore diameter was obtained.

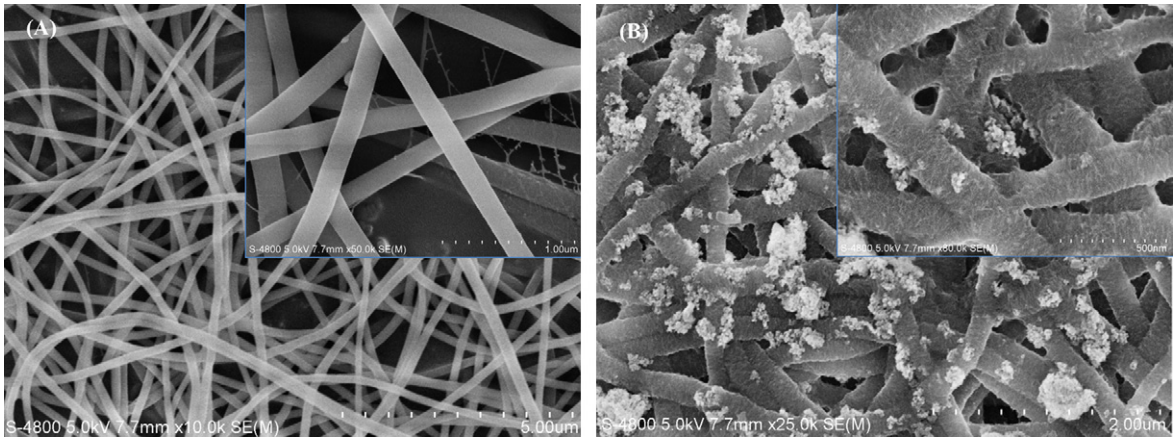

Fig. 2. SEM image of MWNTs–PA6 composite nanofibers (A) and MWNTs–PA6–PPy electrode (B). The inset shows partial surface morphology of the fibers.

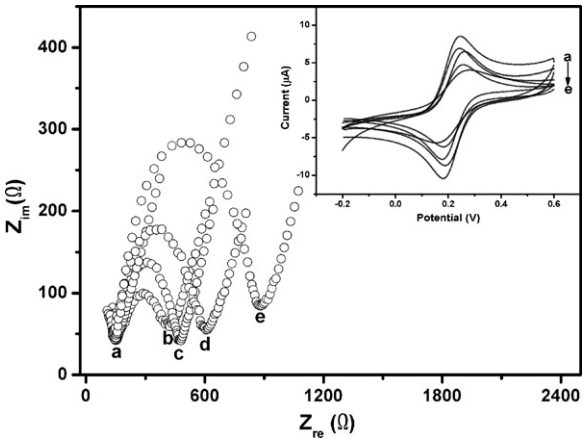

Fig. 3. Nyquist plots for the impedance measurement in 10 mM $[Fe(CN)_6]^{3-/4-}$ solution for the MWNTs–PA6–PPy electrode (a), bare Au electrode (b), MWNTs–PA6 electrode (c), ssDNA electrode (d) and dsDNA electrode (e). Inset: the corresponding cyclic voltammogram curves in 1 mM $[Fe(CN)_6]^{3-/4-}$ solution. Scan rate: 0.1 V s^{-1}, scan range: 0.0–1.2 V.

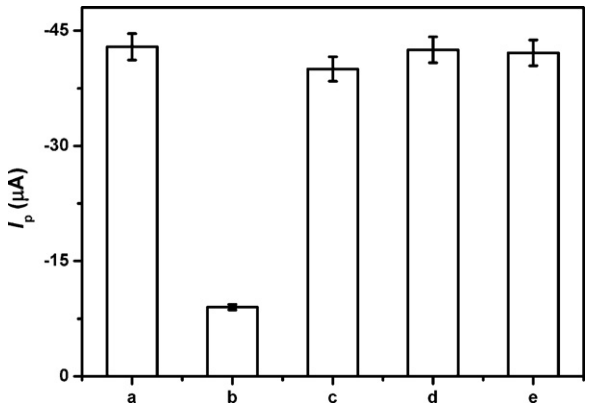

Fig. 4. DPV responses for ssDNA electrode and various dsDNA–MB electrodes. (a) ssDNA electrode, and the concentrations of wtp53 were (b) 20 nM wtp53, (c) 20 nM three-base mismatched sequence of the wtp53, (d) 20 nM noncomplementary sequence of the wtp53 and (e) blank. DPV were achieved in 40 mM Tris–HCl (pH 8.0, 20 mM NaCl). Pulse amplitude 0.05 V, pulse width 0.05 s, and pulse period 0.2 s.

3.2. EIS behavior of different modified electrodes

The fabrication processes of electrochemical biosensor were characterized by electrochemical impedance spectroscopy (EIS). For EIS measurements $[Fe(CN)_6]^{3-/4-}$ was utilized as the redox probe and Nyquist plots were used to calculate the R_{et} for modified electrodes. As shown in Fig. 3, the R_{et} for bare Au electrode was 258.5 Ω (curve b), and increased to 327.9 Ω for the MWNTs–PA6 electrode (curve c). It is consistent with the fact that a trace amount of MWCNTs had not affect on the conductive of the PA6, but MWCNTs could increase the mechanical stability of nanofibers, and make them more durable under operating conditions [34,35]. Nevertheless, the R_{et} of MWNTs–PA6–PPy electrode decreased dramatically to 16.7 Ω (curve a). This reflects the outstanding charge-transport characteristics of the PPy, which might greatly promote electron-transfer reactions of the electrode surface. Once the ssDNA was adsorbed onto the MWNTs–PA6–PPy electrode by electrostatic interactions, the R_{et} increased to 469.7 Ω as shown in curve d. It was resulted in the fact that the ssDNA, which have a single strand nucleic acid with negative charges on its phosphate backbone, makes an electrostatic repulsive force to $[Fe(CN)_6]^{3-/4-}$. When the dsDNA electrode was formed, the increase of the amount of nucleic acid made a stronger repulsive force to $[Fe(CN)_6]^{3-/4-}$. As a result, the R_{et} was changed to 737.6 Ω (curve e). The corresponding CV curves of the electrodes were shown in the insert of Fig. 3. The change in the R_{et} and the CV curves of the electrodes illustrated the successful modification of the functional composite nanofibers onto Au electrode. It also indicated that the interactions between the ssDNA and the p53 gene arose successively.

3.3. The characterization of the electrochemical biosensor

Herein, the binding specificity of the ssDNA electrode was investigated by the control hybridization experiments for wtp53 (complementary sequence of the ssDNA), three-base mismatched sequence of the wtp53, noncomplementary sequence of the wtp53 and the blank. As shown in Fig. 4, the largest DPV peak current (I_p) of MB at −0.32 V was found for the ssDNA electrode (Fig. 4a), while a strong decrease of I_p was detected when the ssDNA electrode was incubated with wtp53 (Fig. 4b). It indicated that the dsDNA has successfully formed and the interaction of MB to guanine residues is prevented by duplex formation, due to the guanine bases have formed hydrogen bonds with cytidine in dsDNA. Therefore, MB, a phenothiazine dye as electrochemical indicator in DNA biosensor, can specifically recognize ssDNA and dsDNA [37–40]. A slight decrease of I_p was obtained when the ssDNA electrode was hybridized with the three-base mismatched sequence (Fig. 4c). When the ssDNA electrodes were hybridized with the noncomplementary sequence of the wtp53 (Fig. 4d) and the blank (Fig. 4e), the corresponding I_p were similar to that of the ssDNA electrode. The consistent data was got when the experiment was repeated three times. The results show that the MWNTs–PA6–PPy-based DNA hybridization assay has high selectivity from the noncomplementary and the three bases mismatch sequence. The relative standard deviation (RSD) of the I_p for the 6 repeated detections of wtp53 (20 nM) was 5.01%, indicating the good reproducibility of this method. The stability of the ssDNA electrode was investigated after 10 days storage at 4 °C and further used to hybridize with the target wtp53 sequence, 96.7% of the initial sensitivity remained, indicating this modified electrode was a stable platform as electrochemical DNA biosensor. Compared to the results of the electrochemical p53 detection presented in earlier reports [21,22], the novel electrochemical biosensor has demonstrated good performance including higher binding specificity, long shelf life and excellent reproducibility.

The electrochemical surface area has been evaluated according to the reported protocols [20]. As shown in Table 1, the electroactive surface area was found to be 0.0314, 0.096 and 0.251 cm^2 for the bare Au, PPy and MWNTs–PA6–PPy electrodes (The Py electropolymerization process of the PPy electrode was the same as the MWNTs–PA6–PPy electrode and the concentration of Py was also same), respectively. Compared with the bare Au electrode, the electrochemical surface area of the PPy electrode significantly improved. It is consistent with the fact that polypyrrole (PPy) film with positive charged 3D porous structure produced by the electropolymerization of the Py can increase the electrochemical surface area effectively [41]. The electrochemical surface area of the MWNTs–PA6–PPy electrode has a significant increase in contrast to the PPy electrode. It is because that each MWNTs–PA6 composite nanofibers having a large surface area can be regarded as an independent micro electrode when the

Table 1
Performance comparison of various electrodes.[a]

Parameter	Bare Au	PPy/Au	MWNTs–PA6–PPy/Au
A (cm^2)	0.0314	0.096	0.251
Discrimination (%)	28.6	39.9	57.5

[a] Wtp53 (20 nM), Mtp53 (20 nM).

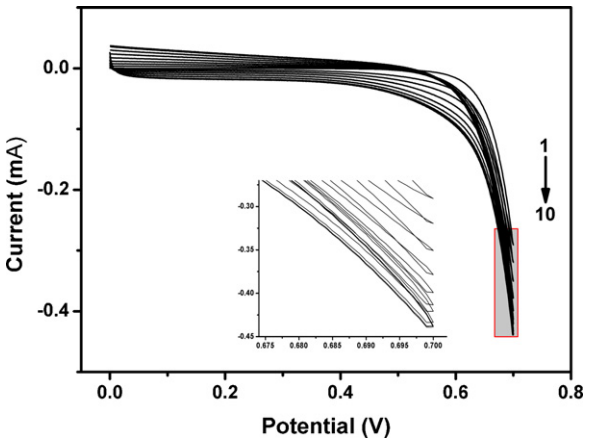

Fig. 5. The cyclic voltammograms of Py electropolymerization with MWNTs–PA6 electrode in 0.05 M Py solution containing 0.1 M KCl–HCl (pH 3.0) for 10 cycles. Scan rate: 50 mV s^{-1}, scan range: 0.0 to +0.7 V. Inset: the partial enlargement graph.

electropolymerization reaction taken place on the MWNTs–PA6 electrode. By this way, a significantly increasing of the PPy amount around MWNTs–PA6 composite nanofibers was achieved. Finally, the MWNTs–PA6–PPy electrode with larger electrochemical surface area was obtained. Herein, the binding specificity of the bare Au, PPy and MWNTs–PA6–PPy electrodes were investigated by the control hybridization experiments for wtp53 and mtp53. The signal of mtp53 (C/T mismatched) turns out to be about 28.6%, 39.9% and 57.5% of that of the wtp53 for the bare Au, PPy and MWNTs–PA6–PPy electrodes in the same concentration. In other words, the discrimination of wtp53 and mtp53 are 28.6%, 39.9% and 57.5% using the above three electrodes (Table 1). The consistent data was obtained when the experiment was repeated three times. The results benefit from the unique 3D nanostructure (as shown in Fig. 2B), large specific surface area and good biocompatibility of MWNTs–PA6–PPy electrode which can dramatically increase the amount of ssDNA attachment and hybridization sensitivity.

3.4. Optimization of experimental conditions

In order to maximize the detection sensitivity of the proposed electrochemical biosensor, various conditions were optimized by single factor experiments. In 3 min, the MWNTs–PA6 nanofibrous mat was deposit on the surface of the Au electrode, and was visible directly. The cycles of CV for Py electropolymerization were investigated. As shown in Fig. 5, with the increase of the scan cycle number, scanning current gradually increased, and increased slowly after 8 cycles. For conventional studies, the performance of conducting polymer is strongly influenced by the thickness of the polymer film. Increasing the film thickness will deteriorate the hybridization detection sensitivity [41]. In consideration of the analysis time and sensitivity, we employed 8 cycles of CV in range of 0.0 to +0.7 V for Py electropolymerization with scan rate of 50 mV s^{-1}.

The efficiency of the hybridization is in correlation with the ionic strength of the hybridization buffer, hybridization time and hybridization temperature. The DPV peak current (I_p) of MB at −0.32 V decreased with the increasing of the NaCl concentration and the hybridization time. It reached plateau regions at the NaCl concentration of 0.5 M and the hybridization time of 40 min as shown in Fig. 6A and B. Thus, the optimal NaCl concentration and hybridization time were chosen at 0.5 M and 40 min. The curve that the ECL intensity varied with the hybridization temperature from 20 °C to 50 °C with an increment of 5 °C was like a parabola and its peak was at 40 °C as shown in Fig. 6C. So, 40 °C was chosen as the optimal hybridization temperature.

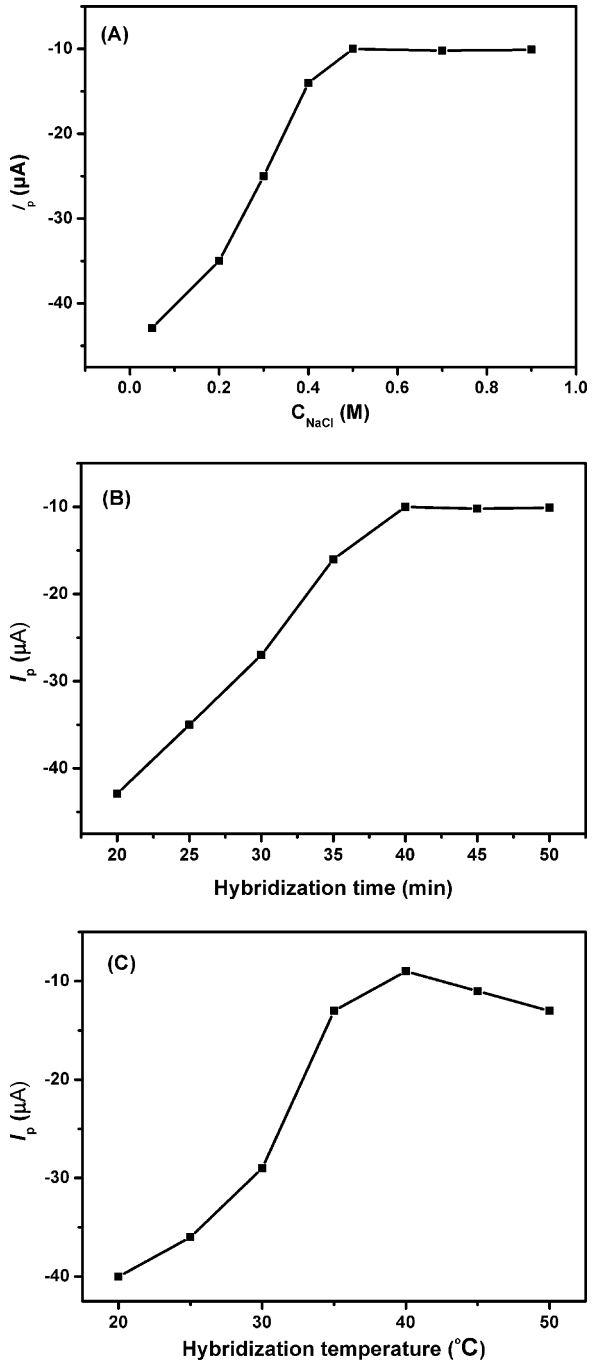

Fig. 6. Effects of the hybridization conditions on the I_p of MB. (A) The hybridization buffer solution, (B) the hybridization time and (C) the hybridization temperature.

In order to accumulate MB onto dsDNA, the MB concentration in the 50 mM Tris–HCl (pH 8.0) were chosen at 20 μM according to the Ozkan group's studies [42,43]. The incubation time of the dsDNA electrode with MB was explored. With the incubation time increased, the I_p decreased rapidly and reached a plateau after 8 min as shown in Fig. 7. It meant that the binding was almost completed after 8 min. So, we employed 8 min as the incubation time.

In addition, the ionic strength condition of the detecting Tris–HCl buffer solution has great impact on the I_p of MB at −0.32 V. It was affirmed that positively charged MB was electrostatically attached to the negatively charged phosphate backbone of dsDNA at low ionic strength conditions. In a high ionic strength solution (after 10 mM NaCl in Tris–HCl buffer solution), majority of the MB

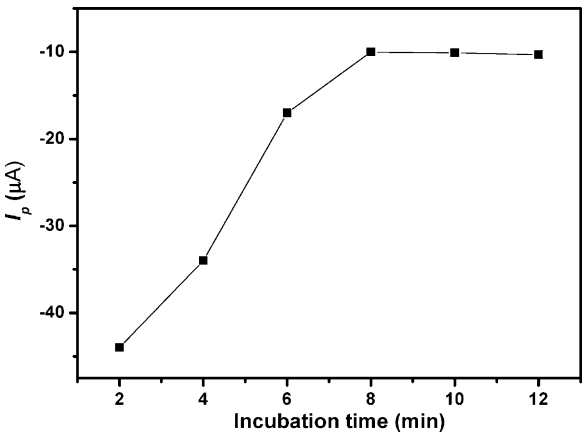

Fig. 7. Effects of the incubation time on the I_p of MB in 50 mM Tris–HCl (pH 8.0, 20 μM MB).

molecules started intercalating between the double helix of dsDNA, because the ionic shielding of the negative charges on the DNA was established. The amount of the NaCl concentration of the detecting Tris–HCl buffer solution was selected according to the literature [42,43]. So, 40 mM Tris–HCl (pH 8.0, 20 mM NaCl) was selected as the DPV detecting solution.

3.5. The calibration curve of wtp53 detection

The sensitivity of the electrochemical biosensor was investigated. DPV responses for various dsDNA–MB electrodes are shown in Fig. 8. The peak currents difference (ΔI_p, $\Delta I_p = I_p(\text{ssDNA}) - I_p(\text{dsDNA})$) of MB reduction grew when the wtp53 concentration increased, and the ΔI_p was found to be linear with the logarithm of wtp53 concentration in the range from 0.1 pM to 100 pM (as shown in the inset). The equation for the resulting calibration plot was $y = -3.62\lg x - 10.12$ (x was the concentration of wtp53, y was the ΔI_p), correlation coefficient was 0.9992. The detection limit for wtp53 of 50 fM was estimated using 3σ (where σ is the relative standard deviation of a blank solution, $n = 11$), which is comparable or better than that in reported p53 assays [14,15,22]. The consistent data was obtained as shown in the error bar in the inset of Fig. 8 when the experiment was repeated three times.

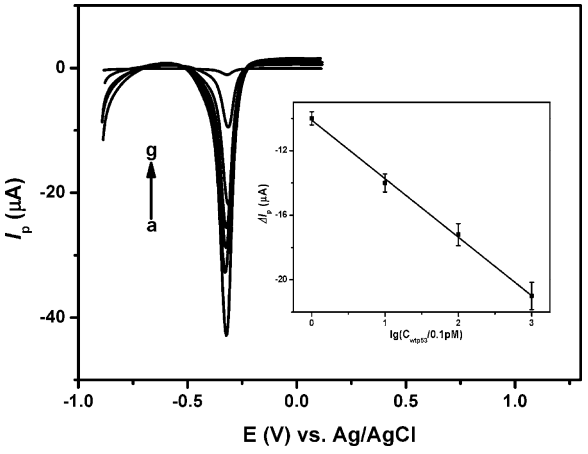

Fig. 8. DPV responses for various dsDNA–MB electrodes. The concentrations of wtp53 were (a) 0.00, (b) 0.1 pM, (c) 1 pM, (d) 10 pM, (e) 100 pM, (f) 1 nM, (g) the DPV response of MB for the MWNTs–PA6–PPy electrode with no ssDNA in 40 mM Tris–HCl (pH 8.0, 20 mM NaCl). Inset: related calibration plot vs. wtp53 concentrations in the range from 0.1 pM to 100 pM.

4. Conclusions

An electrochemical biosensor based on functional composite nanofibers for hybridization detection of a specific mutation in the p53 tumor suppressor gene has been designed. The MWNTs–PA6–PPy electrode with unique 3D nanostructure, large specific surface area and good biocompatibility has been proposed and can be used to enhance stability, speed, and sensitivity. MB was chosen as the DNA hybridization indicator in order to develop the sensor by decreasing the nonspecific reaction. The biosensor displayed wide linear range, high sensitivity and good stability. The assay allows detection at levels as low as 50 fM of the wtp53, and the discrimination is up to 57.5% between the wtp53 and the mtp53. Hence, it appears to be a candidate technique for the detection of gene mutation. Moreover, the strategy could be extended to develop various electrochemical biosensors for the detection and quantification of many kinds of analytes, such as DNA/RNA, protein, bacterium, etc.

Acknowledgments

Project supported by the National Important Project on Scientific Research of China (Nos. 2010CB732404 and 2011CB933404), the National Nature Science Foundation of China (Nos. 30972504, 81170492 and 81172721), the Doctoral Program of Higher Education of China (No. 20110092120055), the Innovation Fund of Southeast University (No. 3225000501), the National innovation experimental project of China (Nos. 1210286104 and T12421001) and the Open Research Fund of State Key Laboratory of Bioelectronics of Southeast University.

References

[1] A.J. Levine, J. Momand, C.A. Finlay, Nature 351 (1991) 453–456.
[2] L.J. Hofseth, S.P. Hussain, C.C. Harris, Trends Pharmacol. Sci. 25 (2004) 177–181.
[3] K.H. Vousden, D.P. Lane, Nat. Rev. Mol. Cell Biol. 8 (2007) 275–283.
[4] P. Hainaut, K.G. Wiman, Lancet Oncol. 10 (2009) 913–919.
[5] M. Olivier, M. Hollstein, P. Hainaut, Cold Spring Harb. Perspect. Biol. 2 (2010) a001008.
[6] K. Will, G. Warnecke, S. Bergmann, W. Deppert, Nucleic Acids Res. 23 (1995) 4023–4028.
[7] G. Narayanaswami, P.D. Taylor, Genet. Test. 6 (2002) 177–184.
[8] K. Miyajima, S. Tamiya, Y. Oda, T. Adachi, T. Konomoto, H. Toyoshiba, K. Masuda, M. Tsuneyoshi, Cancer Lett. 164 (2001) 177–188.
[9] N.J. Van Orsouw, R.K. Dhanda, R.D. Rines, W.M. Smith, I. Sigalas, C. Eng, J. Vijg, Nucleic Acids Res. 26 (1998) 2398–2406.
[10] T. Jiang, M. Minunni, M. Mascini, Clin. Chim. Acta 343 (2004) 45–60.
[11] D. Potesil, R. Mikelova, V. Adam, R. Kizek, R. Prusa, Protein J. 25 (2006) 23–32.
[12] K.A. Gould, C. Nixon, M.J. Tilby, Mol. Pharmacol. 66 (2004) 1301–1309.
[13] G. Gupta, P. Atanassov, Electroanalysis 23 (2011) 1615–1622.
[14] E. Farjami, L. Clima, K. Gothelf, E.E. Ferapontova, Anal. Chem. 83 (2011) 1594–1602.
[15] E. Paleček, V. Ostatná, H. Černocká, A.C. Joerger, A.R. Fersht, J. Am. Chem. Soc. 133 (2011) 7190–7196.
[16] A. Tiwari, S.R. Deshpande, H. Kobayashi, A.P.F. Turner, Biosens. Bioelectron. 35 (2012) 224–229.
[17] C.P. Chen, A. Ganguly, C.Y. Lu, T.Y. Chen, C.C. Kuo, R.S. Chen, W.H. Tu, W.B. Fischer, K.H. Chen, L.C. Chen, Anal. Chem. 83 (2011) 1938–1943.
[18] F. Domenici, A.R. Bizzarri, S. Cannistraro, Anal. Biochem. 421 (2012) 9–15.
[19] L.P. Qiu, Z.S. Wu, G.L. Shen, R.Q. Yu, Anal. Chem. 83 (2011) 3050–3057.
[20] X.Y. Wang, X.Y. Zhang, P.G. He, Y.Z. Fang, Biosens. Bioelectron. 26 (2011) 3608–3613.
[21] J.P. Tosar, G. Branas, J. Laíz, Biosens. Bioelectron. 26 (2010) 1205–1217.
[22] J.B. Raoof, R. Ojania, S.M. Golabib, E. Hamidi-Asla, M.S. Hejazi, Sens. Actuators B: Chem. 157 (2011) 195–201.
[23] Z.G. Wang, L.S. Wan, Z.M. Liu, X.J. Huang, Z.K. Xu, J. Mol. Catal. B: Enzym. 56 (2009) 189–195.
[24] S.H. Jiang, H.Q. Hou, A. Greiner, S. Agarwal, Appl. Mater. Interfaces 4 (2012) 2597–2603.
[25] S. Huang, Y. Ding, Y.X. Liu, L. Su, R. Filosa Jr., Y. Lei, Electroanalysis 23 (2011) 1912–1920.
[26] Q. Xu, N.P. Zhang, X.Y. Yin, M. Wang, Y.Y. Shen, S. Xu, L. Zhang, Z.Z. Gu, J. Chromatogr. B 878 (2010) 2403–2408.
[27] M. Maas, P. Guo, M. Keeney, F. Yang, T.M. Hsu, G.G. Fuller, C.R. Martin, R.N. Zare, Nano. Lett. 11 (2011) 1383–1388.

[28] N. Naveen, R. Kumar, S. Balaji, T.S. Uma, T.S. Natrajan, P.K. Sehgal, Adv. Eng. Mater. 12 (2010) B380–B387.
[29] S. Marx, M.V. Jose, J.D. Andersen, A.J. Russell, Biosens. Bioelectron. 26 (2011) 2981–2986.
[30] M. Ahmad, C.F. Pan, Z.X. Luo, J. Zhu, J. Phys. Chem. C 114 (2010) 9308–9313.
[31] S.J. Lee, R. Tatavarty, M.B. Gu, Biosens. Bioelectron. 38 (2012) 302–307.
[32] X.X. Wang, T. Yang, X. Li, K. Jiao, Biosens. Bioelectron. 26 (2011) 2953–2959.
[33] N.G. Karsli, T. Yilmaz, A. Aytac, G. Ozkoc, Compos. Part B: Eng. 44 (2013) 385–393.
[34] J.S. Jeong, S.Y. Jeon, T.Y. Lee, J.H. Park, J.H. Shin, P.S. Alegaonkar, A.S. Berdinsky, J.B. Yoo, Diamond Relat. Mater. 15 (2006) 1839–1843.
[35] Y. Dror, W. Salalha, R.L. Khalfin, Y. Cohen, A.L. Yarin, E. Zussman, Langmuir 19 (2003) 7012–7020.
[36] H.W. Gao, X.W. Qi, Y. Chen, W. Sun, Anal. Chim. Acta 704 (2011) 133–138.
[37] A. Erdem, K. Kerman, B. Meric, U.S. Akarca, M. Ozsoz, Anal. Chim. Acta 422 (2000) 139–149.
[38] D. Ozkan, A. Erdem, P. Kara, K. Kerman, J.J. Gooding, P.E. Nielsen, M. Ozsoz, Electrochem. Commun. 4 (2002) 796–802.
[39] W.R. Yang, M. Ozsoz, D.B. Hibbert, J.J. Gooding, Electroananlysis 14 (2002) 1299–1302.
[40] Z. Chang, H. Fan, K. Zhao, M. Chen, P.G. He, Y.Z. Fang, Electroanalysis 20 (2008) 131–136.
[41] H. Cai, Y. Xu, P.G. He, Y.Z. Fang, Electroanalysis 15 (2003) 23–24.
[42] P. Kara, K. Kerman, D. Ozkan, B. Meric, A. Erdem, Z. Ozkan, M. Ozsoz, Electrochem. Commun. 4 (2002) 705–709.
[43] A. Erdem, K. Kerman, B. Meric, M. Ozsoz, Electroanalysis 13 (2001) 219–223.